The Nitric Acid Hydrates: Ab Initio Molecular Study, and RAIR Spectra of the Solids

R. Escribano,* M. Couceiro, P. C. Gómez,† E. Carrasco,‡ M. A. Moreno, and V. J. Herrero

Instituto de Estructura de la Materia, Consejo Superior de Investigaciones Científicas, Serrano 123, 28006 Madrid, Spain, and Departamento de Química Física, Facultad de Ciencias, Universidad Complutense, Avda. Complutense s/n, 28040 Madrid, Spain

Received: June 7, 2002; In Final Form: October 15, 2002

The molecular complexes formed by nitric acid with one, two, and three water molecules have been investigated by high level ab initio calculations. The B3LYP/aug-cc-pVTZ method and basis set have been used to derive equilibrium geometries and binding energies and to predict the infrared spectra of these complexes. It has been found that the complexes become stable through the formation of several hydrogen bonds. The main one is established between the acid, which acts as a donor, and the first water molecule, but further bonds are created between successive water molecules, with a weaker bond making a closed structure between the last water unit and the acid. Films of nitric acid mono-, di-, and trihydrates (NAM, NAD, and NAT) have been prepared by deposition on a cold surface and annealing to induce crystallization. RAIR spectra have been taken of these films. The spectra are compared to previous investigations, and the assignments of the spectra and the structure of the crystals are discussed. A global good agreement is obtained with previous transmission and RAIR spectra of thin films and extinction spectra of aerosols.

Introduction

The presence of nitric acid hydrates in stratospheric processes has been the reason that has motivated many investigations on these species. It is accepted that hydrates of nitric acid with one and three water molecules are the main components of polar stratospheric clouds (PSC) of type I. We focus in this investigation on two aspects of the nitric acid hydrates: the structure of hydrates with one, two, and three water molecules (NAM, NAD, and NAT, respectively), from the theoretical point of view, on one side, and the infrared spectroscopy of their crystals, on the other side. The complex molecular species are thermodynamically stable with respect to their individual molecular components, and could be produced in rarefied media, such as free jet expansions. For example, the microwave spectrum of the monohydrate, obtained by evaporation of the liquid in a supersonic expansion, has been recently reported.[1] The relevance of the complexes in atmospheric chemistry is still discussed,[2,3] as these loosely bound systems would tend to coalesce into amorphous or crystalline solids under most atmospheric conditions. In the solid state, the monohydrate and trihydrate have been assumed to be the only stable species for a long time, appearing in the nitric acid−water phase diagrams.[4] However, recent experimental evidence by X-ray diffraction[5] has disclosed the structure of the crystal of the dihydrate, confirming the existence of this species, which had been previously anticipated by Ritzhaupt and Devlin[6] from the analysis of the infrared spectra of the solids. The present investigation aims to follow the evolution of the changes in structure and energy as the molecular species are formed by addition of water units to the initial nitric acid monomer. A parallel investigation is presented from the experimental point of view, by discussing the observed changes in the infrared spectra of the crystalline structure of the hydrates.

The previous most relevant theoretical calculations that we have found on these molecules are those of Koller and Hadzi,[7] Tao et al.,[2] Tóth,[8] Sullivan et al.,[9] and Staikova and Donaldson.[10] In the former paper, initial geometries of NAM and NAT were obtained by semiempirical methods, which were followed by Hartree−Fock (HF) calculations with various basis sets, up to 4-31G for full optimization, and 6-31++G** for optimization of intermolecular parameters. Refined geometries and interaction energies, $E_{int} = E_{dimer} - E_{monomer}$, are discussed in that work, as well as the structures of the ionic species, NO_3^- and H_3O^+. At the computing capabilities of that time, they found large variations of the optimized parameters with the basis set employed. In a more recent work, Tao et al.[2] carried out a high level ab initio calculation using MP2 theory and a 6-311++G-(2d,p) basis set, to estimate the optimized geometry of the $HNO_3 \cdot H_2O$ complex, its binding energy, and the possible implications of this species in atmospheric chemistry. Tóth[8] focused his research also on the monohydrate complex, obtaining an optimized geometry and predicting its infrared spectrum, working at different methodologies (semiempirical, HF, second-order Möller−Plesset MP2, and density functional theory, BLYP), and choosing a plane wave basis set. He also investigated the crystal structure using density functional molecular dynamics methods, optimizing the ionic positions of the bulk and the (100) surface of the crystal. Sullivan et al.,[9] on the other hand, studied the trihydrate species, performing an ab initio molecular dynamics calculation to simulate the crystal at atmospherically relevant temperature. In the most recent paper on these systems, Staikova and Donaldson[10] have determined the geometrical structure and binding energy of the nitric acid−water complex by high level computing, using DFT(B3LYP) and 6-311++G(3df,3dp). Their results are very similar to those obtained in this work, and will be discussed in more detail

* Corresponding author. E-mail: rescribano@iem.cfmac.csic.es.
† Universidad Complutense.
‡ Present address: Departamento de Física de Materiales, Facultad de Ciencias Físicas, Universidad Complutense s/n, 28040 Madrid, Spain.

10.1021/jp0262620 CCC: $25.00
Published on Web 01/01/2003

below. It appears that a comprehensive study on these complexes, like the one presented here, has never been reported.

IR spectra of crystalline samples of the nitric acid hydrates have been reported by various groups since the early nineties,[6,11−25] and although the main spectral features have been identified, there is not a full consistency in the published results. Ritzhaupt and Devlin[6] presented the spectra of amorphous thin films deposited at 80 K from mixtures of water and nitric acid vapor. By annealing the appropriate ratios of 1:1, 2:1, and 3:1, they produced the crystalline mono-, di-, and trihydrates and also showed the spectra of these films at 50 and 175 K. Increasing the amount of water beyond the 3:1 proportion did not lead to the formation of any stable crystalline hydrate with higher water content than NAT. Ritzhaupt and Devlin provided also a comprehensive analysis of their transmission spectra, describing the most outstanding peaks in terms of the vibrations of the H_3O^+ and NO_3^- ions and of the stretching bands of the coordinated water molecules. Tolbert et al.[13] and Koehler at al.[12] corroborated essentially the previous data and confirmed the assignment of the spectra to each of the three hydrates, in particular of the one corresponding to the thermodynamically metastable NAD which had led to some controversy,[11] by means of complementary mass spectrometric measurements. In addition, these authors characterized another stable structure of the trihydrate, prevailing at temperatures higher than ≈185 K, which they labeled β-NAT (renaming the previously studied structure as α-NAT). In a later work, Toon at al.[26] presented a comprehensive study of the spectra and optical constants of the amorphous and crystalline nitric acid hydrates.

Reflection−absorption infrared spectra (RAIRS) of thin films of nitric acid hydrates deposited on metallic substrates have also been reported.[15,16,18,19] In the spectra of very thin films (≈100 nm) studied by Koch et al.,[18] the effects of the metallic surface on the deposited layer are significant and as a consequence, some of the peaks observed in transmission are suppressed and others are enhanced due to the "metal surface selection rule". As the film thickness increases, the influence of the metallic surface becomes smaller, bulk effects prevail, and the spectra become closer, though not identical, to those measured in transmission.[6,15,19]

In an attempt to mimic more closely the actual composition of the PSCs, large clusters and aerosols of the nitric acid hydrates were produced at various laboratories.[14,17,20−24] IR extinction spectra of the solid particles were used to monitor condensation and crystallization processes in mixtures of nitric acid and water. Under many circumstances the metastable NAD, having a lower energetic barrier for nucleation than NAT, was observed to form preferentially at the initial stages of the crystallization process. Attempts to form NAM clusters were unsuccessful. Besides, as in the case of thin films, no hydrates higher than NAT were seen. The extinction spectra of NAD and NAT were found to be very similar to the corresponding transmission spectra of thin films. From the extinction spectra of NAT and NAD aerosols, Richwine et al.[17] and Niedziela et al.[22] derived a set of optical constants, which showed some discrepancies with those previously obtained by Toon et al.[26] The authors attributed these discrepancies to the differences between aerosols and thin layers, the latter being affected to a greater or lesser extent by the substrate on which they were deposited. Nevertheless, Tisdale et al.[25] demonstrated in a recent work that significant variations could also be observed between the spectra of aerosol particles (or thin films) of the same nitric acid hydrate recorded under different formation circumstances, and suggested that the "history" of a given sample could be more relevant for the details of the spectrum than the "type" of sample (thin film or aerosol).

Some of the theoretical calculations mentioned above reported the predicted vibrational spectra of the crystalline mono- and trihydrates.[8,9] These calculations provide a reasonable global picture of the measured spectra, but they are limited to the peak positions which are reproduced within an accuracy of about 10%. The calculations do not give the relative band intensities and in some cases lead to assignments which are at variance with the experimental ones.

In this article, we perform a high level ab initio study of the geometrical structure of the clusters of nitric acid and one, two, and three water molecules, and predict their infrared spectra. We present also an experimental investigation of thin films of the corresponding hydrates, prepared inside a temperature-controlled vacuum cryostat, from where their RAIR spectra are measured. The results are discussed and compared to previous works.

Methods

Ab Initio. To investigate the geometrical structure and spectroscopic properties of the nitric acid hydrates, where several hydrogen bonds are present, both correlation energy and basis set effects must be dealt with properly. To provide a description of uniform quality in all these systems, while keeping computational effort at a reasonable level in the most complex clusters, a triple-ζ plus polarization basis set (TZP) seems an advisable choice. Previous exploratory calculations performed using the correlated consistent cc-pVDZ basis set lead to the conclusion that the water monomers situated farther away from the nitric acid, which are more weakly bound to the rest of the molecule, have some distorted configuration, reaching for example a value of 102.30° for the HOH angle. Therefore we have used throughout this paper cc-pVTZ and aug-cc-pVTZ basis sets, where this type of distortions are much reduced. It has been observed that the inclusion of diffuse functions plays a role in the intermonomeric parameters, especially in the case of bond angles; for example, the hydrogen bond angle O−H···O in NAM increases its value by 1° upon the inclusion of diffuse functions. Also, variations in the hydrogen bond distances are found, producing changes normally in the second decimal place in angstroms. In contrast with this, virtually no changes in the intramonomeric bond distances and angles are observed, this being an interesting exception to the case of the dihedral angle O1−N−O3−H. This dihedral angle has values very close to 180° both in NAM and NAD, but surprisingly enough goes far from planarity (ca. 169°) in NAT when using cc-pVTZ basis set; however, this behavior is somewhat corrected by the inclusion of diffuse functions that predict a value close to 176°. It was also found that the effect of diffuse functions becomes larger as the cluster becomes more complex. On the other hand, basis set improvements beyond aug-cc-pVTZ will likely have little effect on most geometrical parameters, as was the case in $(H_2O)_3$.[27] As a consequence of the considerations above, we have chosen aug-cc-pVTZ as the basis set of work to which all the results provided in this paper refer.

The treatment of correlation in the present type of clusters linked by medium-strength hydrogen bonds, where dispersive effects are not likely to be important, can be carried out in an efficient manner by using DFT methods. In particular, the non local three-parameter hybrid functional B3LYP has proved its reliability when used along with TZP+ diffuse functions basis set in a variety of molecular properties of dimers linked by hydrogen bond,[28,29] being moreover B3LYP a size consistent

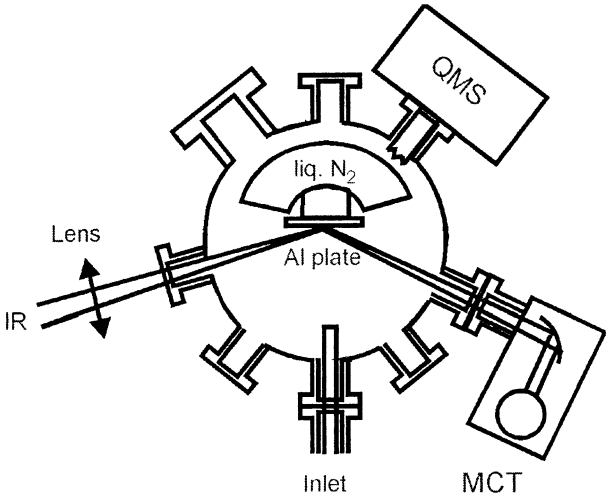

Figure 1. Schematic drawing of the experimental setup. QMS: Quadrupole Mass Spectrometer; MCT: Mercury Cadmium Telluride detector.

method. Optimization of energies and molecular properties calculations have been carried out using the Gaussian 98 suite of programs.[30] Several initial geometries were tried in every case, taken from previous publications where available,[8] or calculated using low level optimization procedures.

The optimized energy of each molecular species was first corrected by the zero-point energy (ZPEC), estimated from the vibrational wavenumbers calculated at the optimized geometry of the monomers:

$$E_{ZP} = E_{opt} + E_{ZPEC}$$

The energy of the hydrates was then corrected from basis set superposition error:

$$E_n = E_{ZP} - E_{CC}$$

The basis set superposition error was taken into account using counterpoise corrections:[31]

$$E_{CC} = \Sigma_i E^*_i(c) - \Sigma_i E^*_i$$

Here $E^*_i(c)$ represents the energy of the monomer (water or nitric acid) calculated using the basis set of the whole cluster and the geometry of the monomer in the cluster, and E^*_i indicates the energy of the monomer, with the same geometry, but with its own basis set. From these values, we have calculated binding energies with reference to the nitric acid and water isolated molecules. The energy difference was obtained from the calculated results at the equilibrium position in the way:

$$E_{bind} = E_n - E_{HNO_3} - nE_{H_2O}$$

Experimental Section

Solid films of nitric acid hydrates were formed by deposition of suitable mixtures of HNO_3 and H_2O vapors on the cold surface of a cryostat built in our laboratory. A complete description of the experimental setup is given elsewhere;[32] we will outline here just the most important features. A schematic diagram of the experimental setup is shown in Figure 1. The cold deposition surface is made of polished Al and is placed inside a vacuum stainless steel chamber evacuated by means of a turbomolecular pump. The deposition temperature can be regulated between 80 and 323 K, with an accuracy better than 1 K by controlling the heat flow balance between a liquid nitrogen Dewar and a power transistor in contact with the Al plate. The background pressure of the chamber after filling the liquid nitrogen reservoir and before depositing the ice films was in the 10^{-9} mbar range. Mixed vapors with HNO_3:H_2O approximate ratios 1:1, 1:2, and 1:3 in equilibrium with the corresponding aqueous HNO_3 solutions were allowed into the vacuum chamber through a regulation needle valve. The concentrated HNO_3 solutions needed for the present experiments were prepared at temperatures between 293 and 323 K using standard literature data on HNO_3/H_2O phase equilibria.[33,34] For the deposition of the various ice films the substrate was kept at 85 K and the chamber was filled with a pressure of 2 to 6 $\times$ 10^{-5} mbar (direct ionization gauge reading) of the vapor of interest during 10 to 25 min. The thickness of the films is not known with precision, but assuming a condensation coefficient close to unity for both H_2O and HNO_3, typical values of a few micrometers can be roughly estimated from exposure.[35] The amorphous films obtained at 85 K were then annealed at 175 K in order to induce crystallization. The annealing procedure was continued until no significant variations were observed in the IR spectra which implied typical times of 20−40 min. In the case of the film obtained from the 1:1 mixture, an additional heating of $\approx$5 min at 205 K was necessary. After the annealing, the samples were cooled again to 85 K in order to measure their IR spectra.

The RAIR spectra of the solid films were recorded with a Bruker IFS66 Fourier Transform spectrometer. The source beam of the instrument is extracted from the sample compartment and focused with a CaF_2 lens onto the Al deposition plate at an angle of incidence of 75°. The use of this lens limits the lower end of the available spectral range to $\approx$1000 cm^{-1}. The IR radiation enters and leaves the vacuum chamber through KBr windows. The outgoing IR beam is focused with a mirror on a mercury cadmium telluride (MCT) detector refrigerated with liquid nitrogen. A number of 1024 scans were added for each spectrum, which were measured at 8 cm^{-1} apodized resolution. Spectra measured at different times under the same experimental conditions show a reproducibility of the assigned peaks within a deviation of 20 cm^{-1} in the frequency region below 2000 cm^{-1}, and higher in the upper frequency region, and of the relative intensities within 10−15%. This is a common problem for these crystalline species, as revealed by the dispersion in the values reported by different workers for the same hydrates (see, for example, refs 6,12,15,19, and 25).

Results and Discussion

Equilibrium Geometry of the Complexes. Table 1 collects the most relevant parameters of the equilibrium configuration of the complexes, determined in this investigation. As mentioned above, these ab initio results have been obtained with the combination of the B3LYP/aug-cc-pVTZ method and basis set. We have carried out a similar calculation for the nitric acid and water molecules and the NO_3^- and H_3O^+ ions, for reference. The corresponding results are also included in the Table 1. We have added a column with previous results for the monohydrate, including those of the experimental work of ref 1. The results of Sullivan et al.[9] for the trihydrate, which refer to the crystalline structure of the solid, are not included in the table, but will be discussed below.

Figure 2a displays the structure of the monohydrate in the top panel. The oxygen atom of the water molecule is linked to the hydrogen atom of the nitric acid via a fairly strong hydrogen bond, which runs almost along the direction of the O3−H1 bond of the acid. The bond distance and opening of the angle that

TABLE 1: Optimized Structural Parameters of the Nitric Acid Hydrates Studied in This Work[a]

	$HNO_3(H_2O)$		$HNO_3(H_2O)_2$	$HNO_3(H_2O)_3$		
parameters	this work	prev. works	this work	this work	HNO_3/H_2O	NO_3^-/H_3O^+
			HNO_3 Unit			
N−O1	1.197	1.216[b]	1.198	1.200	1.192	1.258
N−O2	1.219	1.231[b]	1.224	1.225	1.208	1.258
N−O3	1.381	1.384[b]	1.364	1.357	1.414	1.258
O3−H1	0.997	0.998[b]	1.013	1.021	0.972	
O1−N−O2	128.29		127.12	127.35	130.44	120.
(O1,O2) −N−O3	114.91,116.80		115.34,117.55	115.93,116.72	113.92,115.64	120.
N−O3−H1	105.24	104.11[b]	107.98	107.12	103.10	
O1−N−O3−H	179.67		−179.55	176.15	180	
			1st H_2O unit			
O4−H, O4−H′	0.966,0.962	0.970[b],0.966[b]	0.982,0.962	0.990,0.961	0.962	0.980
H−O4−H′	106.66	105.36[b]	107.07	106.57	105.10	112.78
			2nd H_2O unit			
O5−H, O5−H′			0.968,0.962	0.981,0.961		
H−O5−H′			106.36	106.01		
			3rd H_2O unit			
O6−H, O6−H′				0.969,0.961		
H−O6−H′				106.40		
			Hydrogen Bondings			
H1···O4	1.707	1.702[c],*1.779*[d]	1.615	1.571		
O3−H1···O4	173.96	174.59[b],*174.5*[d]	171.99	172.85		
H(O4)···O5			1.765	1.712		
O4−H···O5			162.24	177.92		
H(O5)···O6				1.783		
O5−H···O6				172.12		
O2···H(O4,5,6)	2.406	2.386[c],*2.30*[d]	2.025	1.967		
O2···H−O(4,5,6)	112.79	108[e],*119.3*[d]	152.43	150.15		
			Intermol. Param.			
O3- - -O4	2.700	2.708[c]	2.621	2.588		
O4- - -O5			2.717	2.701		
O5- - -O6				2.759		
O6- - -O2				2.848		
O3−O4−O5			100.70	118.65		
O4−O5−O6				106.81		
O5−O6−O2				81.33		
			Rotat. Constants			
A	12.27	12.31[d]	4.79	2.35	13.07/824.8	13.31/331.0
B	2.72	2.69[d]	1.66	1.18	12.06/429.8	13.31/330.7
C	2.24	2.21[d]	1.24	0.80	6.27/282.6	6.65/188.0
dipole moment	4.158		3.770	3.565	2.261/1.847	0/1.396
optimized energy	−357.4880145		−433.9692705	−510.4493556	−281.0071074/ −76.4661965	−280.4817904/ −76.7385183

[a] The ab initio calculations have been carried out with the B3LYP method and the aug-cc-pVTZ basis set. Distances are in Å, angles in degrees, rotational constants in GHz, dipole moments in Debye, and energies in Hartree (1 Hartree: 2626.5 kJ mol^{-1}). [b] Ref 8. [c] Ref 10. [d] Ref 1. Values are shown in italic to indicate that they correspond to experimental measurements. [e] Ref 2.

usually characterize a hydrogen bond have values of 1.707 Å and 173.96°, respectively. With respect to the isolated HNO_3 unit, the O3−H1 bond of the acid is thus elongated by nearly 0.03 Å. Consequently, the N−O3 bond is shortened by more than 0.03 Å, the ONO angles are rearranged, and the NO_3 group evolves toward a 3-fold symmetry, corresponding to the NO_3^- anion. The dihedral angle of the HNO_3 unit is kept close to 180°, as in the isolated molecule. One of the O−H bonds of the water monomer (labeled O4−H′; in this paper we have used the convention of designating H′ the hydrogen atoms not participating in hydrogen bonding, situated out of the molecular plane) is projected above the plane which contains the rest of the molecule ($z_{H'} = 0.67$ Å, whereas all other atoms are enclosed within 0.1 Å above or below the *xy* plane). A second, weaker hydrogen bond is established between the in-plane H atom of the water unit and the closer oxygen atom (O2) of the nitric acid monomer, with values of 2.406 Å and 112.79° for the bond distance and bond angle, respectively. The water unit acts as a proton donor in this second hydrogen bonding, with the result that the in-plane O4−H bond is slightly longer than the protruding O4−H′. At the same time, the angle of the water unit opens up by 1.5° with respect to the free molecule.

In the first stages of the calculations, with a smaller basis set, a different structure was also obtained for this complex, in which the water unit approached the NO_2 moiety of the nitric acid, being stabilized by the electrostatic attraction between one hydrogen atom of the water and the two oxygens of the NO_2. However, this structure was energetically much less favored than the one depicted in Figure 2a (by nearly 50 kJ/mol), and moreover convergence to this alternative structure was not achieved when using the full basis, hence we will not pursue this subject here.

The third column of Table 1 contains the results of several previous investigations on NAM. For ref 8, we have chosen to quote the results obtained at MP2/cc-pVDZ level, instead of those at BLYP/cc-pVDZ level, because the agreement with our own B3LYP/aug-cc-PVTZ is much better, the differences being probably attributable to insufficiencies in the basis set used in

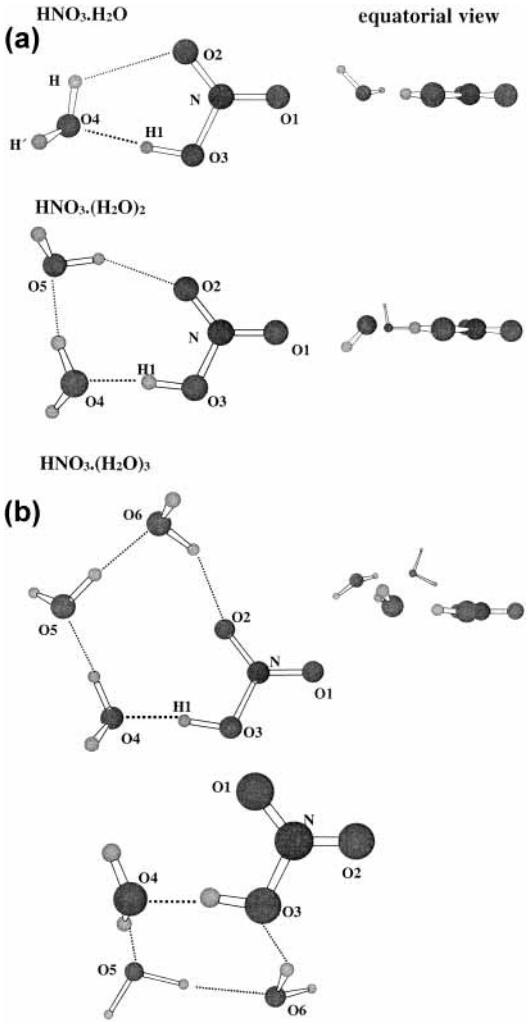

Figure 2. (a) Schematic representation of the molecular complexes studied. Top: monohydrate, showing atom labeling scheme used in this work. Middle: dihydrate. Bottom: trihydrate. On the right are shown views from the plane of the nitrate ion. (b) Schematic representation of the alternative structure found for the trihydrate complex.

ref 8. The comparison of our results with those obtained using BLYP along with a plane wave (PW) basis set[8] is somewhat more complex because of the differences in the methodology, but it seems that BLYP/PW overestimates bond lengths by almost 5% whereas the angles have similar values. However, the agreement of our results with those of ref 10, at B3LYP/6-311++G(3df,2pd) level, for the main hydrogen bond parameters, is very good. Finally, it is very encouraging the excellent agreement between our predicted rotational constants and the experimental ones, shown in italic in the table, with differences within 1% of the experimental values. Thus, we can expect that our predictions for the complexes with two and three water molecules will be reasonably accurate.

The dihydrate is depicted in the middle section of Figure 2a. The strongest hydrogen bond is formed as before between the nitric acid hydrogen and the first water monomer (H1···O4), with 1.615 Å and 171.99° as bonding parameters. Each water unit takes part in two hydrogen bonds, being at the same time donor and acceptor with the consecutive monomers. The corresponding parameters have values that reflect the increasing weakness of the bondings: H(O4)···O5 = 1.765 Å, O4−H−O5 = 162.24° for the first one between the two water monomers, and H(O5)···O2 = 2.025 Å, O5−H−O2 = 152.43° for the second, which closes the ring of bonds with the nitric acid unit. These bonds stabilize the molecule within a plane, out of which are left one O−H bond of each water monomer, one above and one below the molecular plane, as shown in the figure. The same effect of a trend toward a symmetric NO_3^- structure as in the monohydrate is found for the dihydrate. The dihedral angle is still nearly 180°. The first water monomer is more distorted in this case, but the second water unit is only slightly perturbed from the free molecule. Since we have not found any previous calculations on the structure of this dihydrate, we can only compare our results with the experimental determinations for the solid. This will be done below. As in the monohydrate case, a second alternative of this complex was found with a shorter basis set. In this case, the structure was based on that of the monohydrate in Figure 1, with the second water unit linked to the O1 atom, at the opposite end of the molecule with respect to the first water monomer. Again, the energy was about 50 kJ/mol less negative, and again convergence was not reached for the full basis set.

Finally, the trihydrate is shown in the bottom panel of Figure 2a. The HNO_3 unit is almost planar, with a HNO_3 dihedral angle of 176.15°, but the rest of the molecule has lost the planarity of the previously studied species. As before, there is a strong hydrogen bonding between the H1 atom of the nitric and the oxygen of the first water unit, O4. This H1···O4 hydrogen bond is the strongest in these hydrides, as indicated by the longest O3−H1 and the shortest H1−O4 distances. The configuration of the NO_3 group follows the trend toward a symmetric 3-fold structure found in the mono- and dihydrates. The third water unit is linked to the second, and to the O2 atom of the nitric part, closing the ring structure with 10 atoms involved. The nonplanarity of this ring can be observed in the equatorial view at the right of Figure 2a. However, the hydrogen bondings formed in this species are stronger than those in the previous molecules, giving an increased stability to the trihydrate. The water units are also least distorted in the series, except for the longer O−H distances for the H atoms involved in hydrogen bondings.

A second alternative is also found for this cluster, but in this case it does correspond to a stable structure, optimized with the full aug-cc-pVTZ basis set, the energy difference being only 3.2 kJ/mol in favor of that in Figure 2a. The main distinction of this other structure is that the ring of hydrogen bonds is closed on the same O3 atom where it starts, without participation of the rest of the nitric unit. The molecule is depicted in Figure 2b. Also, the hydrogen bondings are slightly weaker and more twisted than in the favored structure. The geometrical parameters for this alternative trihydrate complex are not shown in Table 1 for simplicity, but can be obtained from the authors upon request.

In the optimization process, the convergence was in general quite straightforward for the nitric acid hydrates, both at the lower level used for the initial calculations, and at the higher order level presented here. We did not detect any problems derived from shallow potential surfaces as found sometimes in other hydrogen-bonded species.

It is interesting to examine together the ab initio results and the observations from X-ray diffraction. Although this cannot be a direct comparison, as the forces that are exerted in the crystal on each molecular unit are not paralleled in the theoretical predictions for the isolated species, it is still illustrative to follow the trends in the structure along the series of increasing water content. Table 2 collects the crystallographic results,[5,36,38] and those obtained in this work. The interatomic distances and bond

TABLE 2: Comparison of Experimental X-ray Structures with ab Initio Values Calculated in This Work[a]

		X-ray	this work
NAM			
NO_3^- group	*N−O(av)*[b],N−O3	*1.25*,1.252	*1.21*,1.381
	O−N−O(av),O1−N−O2	*120.0*,120.0	*115.9*,128.3
H_3O^+ group	*O−H(av)*,O4···H1	*0.92*,0.93	*0.96*,1.707
	H−O−H	115	106.7
intermol.	O3- - -O4	2.60[c]	2.70
NAD			
NO_3^- group	*N−O(av)*,N−O3	*1.23*,1.283	*1.21*,1.364
	O−N−O(av),O1−N−O2	*118.6*,122.6	*116.4*,127.1
H_3O^+ group	*O−H(av)*,O4···H1	*0.88*,0.96	*0.97*,1.615
	H−O−H	109	107.1
intermol.	O−O(av)	2.54	2.67
NAT			
NO_3^- group	*N−O(av)*,N−O3	*1.25*,1.244	*1.21*,1.357
	O−N−O(av),O1−N−O2	*120.7*,118.5	*116.3*,127.4
H_3O^+ group	*O−H(av)*,O4···H1	*0.87*,0.82	*0.98*,1.571
	H−O−H	103	106.6
intermol.	O−O(av)	2.60[d]	2.68

[a] B3LYP method and aug-cc-pVTZ basis set. Distances in Å, angles in degrees. X-ray values from Lebrun et al.[5] unless otherwise stated. For NAD the average of A and B structures is quoted. [b] Average values are given for equivalent bonds or angles in italic where indicated. [c] Ref 38. [e] Ref 36.

angles are quoted in italics as averages of the results for equivalent bonds (N−O1 and N−O2, O4−H and O4−H′ in the labeling used in this work), and in straight type for the nonequivalent bonds, involved in hydrogen bonds (N−O3 and O4···H1). The values for the hydronium ion correspond specifically to the units that have this ionic structure in the crystals: all water units are ionic in NAM, whereas in NAD and NAT there exist neutral H_2O units as well, not referenced in this table. It can be seen that the experimental NAM parameters correspond to very symmetric NO_3^- and H_3O^+ groups, whereas in the calculation the N−O3 bond is elongated, with the H1 atom being still linked to the nitrate ion, remaining quite far from the H_2O unit. In the NAD crystal the ionic groups are more asymmetric. This is a consequence of the second hydrogen bond which is formed between the H_3O^+ and the second water molecule, distorting the C_3 symmetry of the ions. The structures of the complexes are closer to the crystals, although the N−O3 and O4···H1 bonds are still longer for the former species. Finally, the crystalline trihydrate structure is peculiar, in the sense that the N−O3 and O4···H1 bonds are shorter than the other two N−O and O−H bonds, with a value of only 0.82 Å for the latter. The NO_3^- geometrical parameters indicate a symmetrical site in the crystal, like that for the NAM. Although the ab initio O4···H1 distance is the shortest one in the series (1.571 Å), it is still much longer than that in the crystal. In summary, the hydrogen bonds formed in the isolated complexes are much weaker than the ionic forces in the crystals, wherein the nitric and water units are completely ionized. Similarly, the interatomic O−O distances are also smaller in the crystalline structures than the predicted values for the complexes, as a result of the packing forces in the solids.

At the bottom of Table 1, the optimized energies of the complexes and the molecular units involved in this investigation are given for reference and comparison. With these values, we have calculated the binding energies for the nitric acid−water clusters, with respect to the isolated HNO_3 and H_2O molecules. The results are collected in Table 3. Similarly to what was found in ref 10 for the monohydrate, the basis set superposition error is almost negligible for these species, amounting to ≈2% of the binding energy, whereas the zero-point energy is larger than

TABLE 3: Binding Energy, Counterpoise Correction, and Zero-Point Energy Correction (kJ/mol) for the Nitric Acid Hydrates Studied in This Work[a]

	E_{bind}	E_{CC}	E_{ZP}
$HNO_3(H_2O)$	−29.31	−0.66	8.66
$HNO_3(H_2O)_2$	−58.58	−1.22	18.36
$HNO_3(H_2O)_3$	−85.59	−1.65	27.38

[a] B3LYP method and aug-cc-pVTZ basis set.

30% of the total. After performing counterpoise and zero-point energy corrections, it can be seen that addition of each water monomer is energetically favorable, increasing the binding energy by about 29, 29, and 27 kJ/mol consecutively. This enhanced stability is a consequence of the creation of multiple hydrogen bonds. The increment is slightly smaller for the trihydrate, which has a nonplanar molecular frame. The planar structure of the other two clusters conveys therefore the idea of a higher stability. Previous estimations of the binding energy of the $HNO_3 \cdot H_2O$ cluster gave values of 30.1 and 31.4 kJ/mol,[2,10] which agree well with the present result. The binding energy of other complexes such as $HOCl \cdot H_2O$ or the water dimer were calculated as 16.8 and 19.6 kJ/mol, respectively.[2,37] These values indicate a higher stability of the nitric acid clusters, in which, both the main hydrogen bond is stronger, and also more than one hydrogen bond is always created. There is an almost constant increase in energy following the addition of progressive water molecules. Whereas the binding of the first water molecule to the nitric acid is the strongest, every new water unit is bonded both to the previous water and to the nitric acid frame, closing in the cyclic structure. It appears that the addition of these two bonds provides an increase in energy similar to that achieved by the first hydrogen-bonding. A fairly similar result was also found along the series of $HOCl \cdot (H_2O)_n$, $n = 1$ to 4.[37]

Predicted Spectra of the Hydrates. We have calculated the infrared spectrum for the optimized equilibrium structure of the molecular complexes studied here, including the individual molecules for comparison. Table 4 presents these results, including a description of the normal mode, and its wavenumber and intensity. The lower frequency vibrations are grouped together under the general label of "intermolecular modes", meaning that it is difficult to make a more accurate description of these modes, where the atoms in the water units are vibrating in different motions and phases. A more intuitive understanding of the spectra is provided in Figure 3, where the predicted spectra are represented as stick lines with heights proportional to intensities normalized to the most intense mode in each spectrum. It is interesting to note that whereas the NO_2 asymmetric stretch and the HOH bend are the most intense bands in the spectra of isolated nitric acid and water, respectively, the strongest vibration in the clusters is always the O3−H1 stretch. This vibration involves the largest charge displacement, since the effect of the hydrogen bonding between H1 and the first water unit is to create a local charge distribution in the sense $O3^-/H1^+$. The shift of this mode to lower frequencies along the series mono-/di-/tri- is a consequence of the lengthening and weakening of the O3−H1 bond, at the same time that the O4···H1 hydrogen bond is becoming stronger. At first sight, it seems that the intensity of the O−H stretches is also reversed from the isolated water, where they are usually labeled antisymmetric (stronger) and symmetric, to the hydrate series, in which the second of these vibrations becomes increasingly strong. When the atomic displacements in each vibration are visualized, it is found that for the hydrates each stretch corresponds to a single O−H bond, and the description based

TABLE 4: Predicted Infrared Spectra of the Nitric Acid Hydrates Studied in This Work[a]

	$HNO_3(H_2O)$	$HNO_3(H_2O)_2$	$HNO_3(H_2O)_3$	HNO_3/H_2O
normal mode				
H_2O str	3874(11)	3867(10)(O5−H′) 3856(6)(O4−H′)	3870(8)(O6−H′) 3857(4)(O5−H′) 3856(4)(O4−H′)	3895(83)
H_2O str	3766(2)	3726(15)(O5−H) 3444(41)(O4−H)	3715(16)(O6−H) 3475(36)(O5−H) 3310(56)(O4−H)	3792(5)
O3−H1 str	3225(100)	2947(100)	2801(100)	3712(23)
NO_2 asym str	1734(26)	1719(13)	1725(9)	1743(100)
H_2O bend	1615(15)	1649(9)(O4) 1625(5)(O5)	1676(7)(O4,O5,O6) 1650(4)(O4,O6) 1630(2)(O4,O5,O6)	1627(100)
H_1NO_3 bend	1468(21)	1471(22)	1497(22)	1315(12)
NO_2 sym str	1324(22)	1327(19)	1330(18)	1341(73)
NO_3 str	939(14)	969(9)	978(6)	896(44)
O3−H1 o−o-pl	867(9)	971(6)	994(6)	480(28)
O−H o−o-pl (H_2O)		857(5)(O4)	926(3)(O4,O5) 804(6) (O4,O5)	
NO_3 o−o-pl wag	794(2)	796(1)	797(3)	783(2)
NO_2 bend	682(0.2)	699(0.2)	698(1)	647(4)
NO_2 rock	643(0.1)	646(1)	667(1)	585(2)
O4−H1 str	221(2)	272(1)	326(4)	
intermol.modes	in pl.427(9) o.o.pl.315(15) o.o.pl.184(5) in pl.101(2) o.o.pl.79(0.1)	532(5),435(10) 314(3), 285(7) 226(7),216(2) 137(0.5),108(0.3) 78(0),23(0)	532(4),493(4),422(5) 320(1),310(5),254(4) 249(4),199(4),192(1) 146(0.2),129(0.5),79(0) 45(0.1),37(0),26(0)	

[a] B3LYP method and aug-cc-pVTZ basis set. Harmonic frequencies in cm^{-1}, and intensities in km mol^{-1} in parentheses.

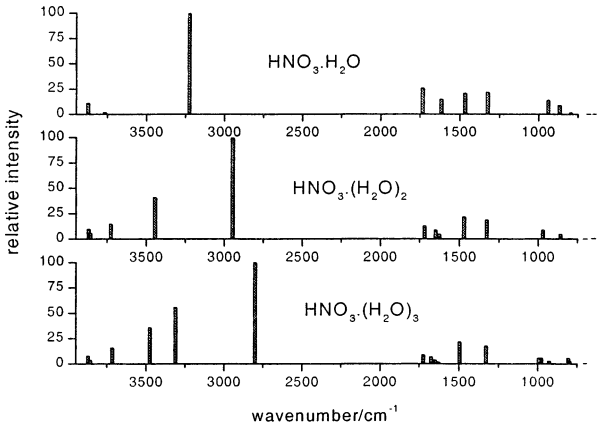

Figure 3. Predicted spectra of the molecular complexes. Infrared intensities are normalized to the most intense line of each spectrum, corresponding to the O3−H1 stretch.

on the symmetry is no longer adequate. The higher frequency, less intense bands correspond to the stretching vibration of the stronger O−H′ bonds, dangling above and below the main plane of the molecule, and the lower frequency, more intense bands are due to the stretching of the weaker O−H bonds, where the H atoms are involved in hydrogen bonding with other oxygen atoms. Their different frequencies in the series of complexes are a consequence of their different environments. The lowest one, in the trihydrate, corresponds to the weakest bond in the water units, which has the longest O−H bond distance in the series (0.990 Å).

The vibrations of the NO_2 and NO_3 units are quite stable in the series of spectra, as much in frequency as in intensity. On the other hand, the O3−H1 stretch and the out-of-plane O3−H1 bend are strongly shifted toward lower and higher frequencies, respectively, as the H1 atom is less tightly linked to the NO_3 part and the hydrogen bonding with the first water unit becomes stronger. Finally, the H_2O bend is also quite stable in the series, with as many bands as water units in each cluster.

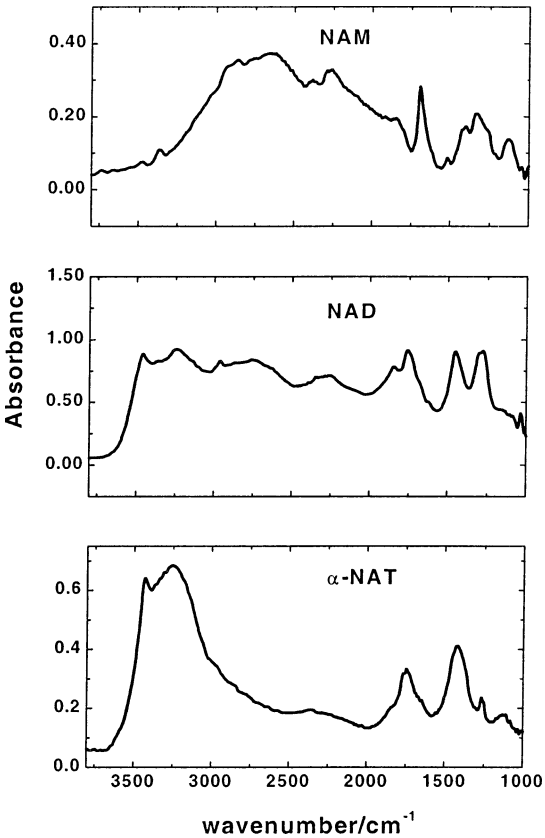

Figure 4. RAIR spectra of nitric acid hydrate films registered in our laboratory. The films have a thickness of the order of micrometerss and were deposited as amorphous solids on a cold metallic substrate and then annealed in order to induce crystallization. Top: NAM, mid: NAD, bottom: α-NAT. The absorbance scale corresponds to base *e* logarithms.

Spectra of the Crystalline Samples. In Figure 4 we display the RAIR spectra of the nitric acid hydrates recorded in our

TABLE 5: Analysis of the Observed Spectra of the Crystals and Comparison with Previous Works, and with ab Initio Results of This Work for the Isolated Species

		$HNO_3(H_2O)$			$HNO_3(H_2O)_2$			$HNO_3(H_2O)_3$		
assignment	pred.[a]	this work	ref 6	ref 19	this work	ref 6	ref 19	this work	ref 6	ref 19
H_2O asym str	3895				3459	3477	3495	3428	3424	3435
H_2O sym str	3792				3241	3215	3265	3251	3203	3220
H_3O^+ asym str	3645	2635	2635	2620	2755	2725	2750	2961sh	2920	2915sh
H_3O^+ sym str	3557	2259	2246	2205	2259	2288	2245	2352	—	2410
H_3O^+ bend $_4$	1672	1693	1674	1664	1841/1757	1829/1693	1734	1743	1753	1765
NO_3^- asym str	1364	1333	1280	1260	1451/1274	1440/1270	1450/1270[b]	1420	1393	1395
H_3O^+ bend ν_2	819	1130	1135	1120[c]	1095sh	1135sh	1174[c]	1119	1110	1128[c]
NO_3^- sym str	1062				1030	1040/1029	1028			

[a] Ab initio prediction for the individual species using the B3LYP method and the aug-cc-pVTZ basis set. [b] Assigned by the authors either to NO_3^- asymmetric stretch or to ν_2 bending mode of H_3O^+. [c] Assigned by the authors to NO_3^- symmetric stretch.

laboratory. From top to bottom ,the spectra correspond to the films obtained by deposition and subsequent annealing of H_2O/HNO_3 vapor mixtures with proportions 1:1, 2:1, and 3:1, respectively. Under the present experimental conditions, these films should correspond essentially to NAM, NAD, and α-NAT, but the presence of amorphous phase or some degree of mixture of the various hydrates in each of the layers cannot be ruled out. The same problem affects also the previous literature spectra of thin layers which have been obtained by comparable procedures.[11−19] The effect of the possible contamination by the other species is, in any case, expected to be small. In Table 5, we have given an interpretation of the main features in the spectra and a comparison with the values of refs 6 (measured in transmission) and 19 (measured in reflection−absorption). The ab initio prediction of the normal modes of isolated H_2O, H_3O^+, and NO_3^- obtained at the optimized geometries calculated in this work are also included in the table.

In the spectrum of the monohydrate, the highest peaks correspond to the stretching vibrations of the hydronium ion at 2635 and 2259 cm^{-1}, respectively, in good agreement with the literature values (note that the peak wavenumbers, here and in the literature, are only approximate, since they usually correspond to broad bands). Between these two maxima, there is a small unassigned peak at about 2383 cm^{-1}, which is also present in the spectra of refs 6, 13, and 19. The peaks of the OH stretching vibrations of water molecules, corresponding to frequencies higher than 3000 cm^{-1}, are absent from the spectrum, since in this crystal all the initial water molecules are incorporated as hydronium ions.[5,38] A shoulder at 2862 cm^{-1} and a small peak at 3361 cm^{-1} can also be seen. Similar features, though less marked, can also be found in the spectra of refs 6, 15, and 19. The frequencies of the stretching vibrations predicted in the present calculations for the isolated H_3O^+ are in good agreement with those from gas-phase literature measurements.[39] The large difference between the frequencies in the gas phase and in the crystal have been attributed to the fact that in the latter the hydronium O−H bonds are weakened because of partial proton transfer from this ion to the NO_3^-.[6] The theoretical ab initio calculations of Tóth[8] give indeed a considerable red shift of the H_3O^+ stretching frequencies in the crystal with respect to those of the isolated ion, but the predicted frequencies are still too high by 300−400 cm^{-1}. At about 1844 cm^{-1} there is a shoulder, also present, but not assigned, in the rest of the published spectra.[6,13,15,19] At 1693 cm^{-1}, the spectrum shows a prominent peak corresponding to the ν_4 bending vibration ("scissors mode") of H_3O^+ in good agreement with literature values.[40] Between 1500 and 1200 cm^{-1} there is a broad absorption with a maximum at 1333 cm^{-1}, which is assigned to the asymmetric stretching, ν_3, of NO_3^-. In addition there is a smaller peak at 1403 cm^{-1} and a shoulder at 1251 cm^{-1} This absorption region is present in the literature spectra,[6,13,15,19] but is concentrated in general around a single maximum at about 1270−1280 cm^{-1}. The RAIR spectrum of Tso and Leu[19] has also two peaks at 1405 and 1230 cm^{-1} at each side of the 1260 cm^{-1} maximum. The presence of peaks or shoulders around the maximum may be an indication of a partial persistence of an amorphous phase, or of some contamination by dihydrate crystals in which the NO_3^- ion would be in an asymmetric surrounding causing a splitting of the otherwise degenerate ν_3 mode. A barely appreciable peak at 1042 cm^{-1} corresponding to the symmetric stretching, ν_1, of the nitrate ion (infrared inactive in a symmetric site) could also have this origin. Finally, the peak at 1130 cm^{-1} appears in the literature at a very similar frequency.[6,13,15,19] In the article of Tso and Leu,[19] this peak (reported at 1120 cm^{-1}) is attributed to the symmetric stretching of NO_3^-, but in general it is assigned to the ν_2 bending vibration ("umbrella mode") of the hydronium ion.

A comparison of the frequencies of the normal modes of the isolated ions (see Table 5 and ref 8) with those assigned to the ions in the three crystalline hydrates shows relatively small variations in the case of NO_3^-. Significant changes are observed, however, in most of the vibrational frequencies of the hydronium ion. Besides the marked red shift in the stretching frequencies already commented on, the umbrella vibration appears in the crystal at a much higher wavenumber than in the isolated ion. The only mode of H_3O^+ whose frequency does not change much upon crystallization is the ν_4 bending.

The spectrum of the dihydrate is characterized, in the frequency range beyond 2000 cm^{-1}, by a continuous absorption with some broad maxima corresponding to the stretching modes of H_2O and H_3O^+. The bands with peaks at 3459 cm^{-1} and at 3241 cm^{-1} are due to the ν_3 and ν_1 stretching modes of the water of hydration, which were absent in the monohydrate as commented on in the previous paragraph. The corresponding modes of the hydronium ion have absorption maxima at 2755 and 2259 cm^{-1}, respectively. The frequencies of all these stretching vibrations, significantly affected by hydrogen bonding, are considerably red-shifted with respect to those of the corresponding modes in the isolated water molecule and H_3O^+ ion (see Tables 4 and 5).

A broad absorption feature with a maximum at 1757 cm^{-1} and a smaller peak at 1848 cm^{-1} is attributed to the ν_4 bending mode of H_3O^+. This feature is observed also in the previous works[6,12,13,15,18,19] and, although its asymmetric shape with a maximum at ≈1700−1750 cm^{-1} is similar in all the spectra, only Ritzhaupt and Devlin[6] identify it as a doublet with components at 1829 and 1693 cm^{-1}. The frequency shift and the splitting of this absorption with respect to the corresponding one in NAM is taken by Ritzhaupt and Devlin as an indication of the influence of hydration. The absorption assigned to the ν_2

mode of hydronium appears now as a small shoulder at about 1150 cm^{-1} in accordance with most of the literature measurements performed on thin films[6,12,13,15] and in the NAD aerosol spectrum recorded by Dieselkamp et al.[20] at 205 K. In the majority of the aerosol spectra,[14,22,23] in the thin film transmission spectrum measured by Ritzhaupt and Devlin at 50 K,[6] and in the RAIR spectrum of Tso and Le,[19] this feature appears as a not very intense peak. Significant changes with respect to the NAM spectrum are observed in the absorptions corresponding to the vibration frequencies of the nitrate ion. The formerly degenerate ν_3 mode of NO_3^- is now clearly split into two distinct maxima at 1451 and 1274 cm^{-1}, and a small but definite peak assigned to the ν_1 stretching appears at 1034 cm^{-1}. In the article of Tso and Leu,[19] the peak at 1174 cm^{-1} is not attributed to the ν_2 mode of water, but to the symmetric stretch of NO_3^-. These authors suggest also that their 1270 cm^{-1} peak may be due not only to a component of the ν_3 mode of NO_3^-, but also to a bending mode of water.

The most characteristic features such as the splitting of the degenerate vibrations (the ν_3 mode of NO_3^- and possibly the ν_4 mode of H_3O^+) and the appearance of a peak corresponding to the infrared inactive ν_1 stretching of the nitrate indicate that the ions, especially NO_3^-, must occupy asymmetric sites in the crystal.[6] Although the dihydrate crystal is not a thermodynamically stable phase, a recent study of its structure using X-ray diffraction[5] has confirmed the perturbation of the NO_3^- symmetry. On the other hand, the observation of somewhat different IR spectra of NAD prepared under different conditions suggests the possible existence of more than one crystal structure.[25]

The spectrum of α-NAT (under our experimental conditions the higher temperature phase of the trihydrate, β-NAT,[13] should not form) is also characterized by strong absorption bands peaking at 3428 and 3251 cm^{-1} due to the stretching modes of the water of hydration. In comparison with the NAD spectrum, these absorption bands are significantly more intense than those of the ν_3 and ν_1 stretching modes of hydronium, which appear now as a shoulder at about 2961 cm^{-1} and as a broad band with a weak maximum at 2352 cm^{-1}. Sullivan et al.[9] have reported ab initio molecular dynamics calculations of the vibrational spectra of NAT at 195 K. At this temperature, the stable phase of the hydrate is β-NAT and our results on α-NAT are not strictly comparable; nevertheless, some of the features, in particular the bands associated with the stretching modes of the water of coordination, should not be too different in the two NAT varieties.[12,13,15,19] The stretching frequencies will be red-shifted and broadened in the crystal as compared with the isolated molecule. (In this respect it is instructive to observe in Table 4 the gradual red shifting and "broadening" of the stretching modes of water with increasing monomer size.) The theoretical calculations of Sullivan et al.[9] overestimate the red shifting of the ν_3 and ν_1 frequencies of H_2O in the NAT crystal by about 300 cm^{-1}.

The spectral features in the 2000−1000 cm^{-1} frequency range indicate that, in the α-NAT crystal, the ions are located in a symmetric environment, in good agreement with the crystal structure determined by X-ray diffraction.[5,36] The peaks at 1743 and 1119 cm^{-1} are attributed to the ν_4 and ν_2 bending modes of H_3O^+. The splitting of the absorption band corresponding to the ν_3 stretching of NO_3^-, observed in the NAD spectrum, is essentially removed in the spectrum of α-NAT, where it appears as a single band peaking at 1420 cm^{-1}. The small peak at 1030 cm^{-1} assigned in the NAD spectrum to the ν_1 mode of the nitrate ion has disappeared from the spectrum of α-NAT. The spectrum of the trihydrate is in good agreement with those published in the literature.[6,12−19,24] The most significant difference between the present and the published data is the frequency shift in the maximum of the ν_3 band of the nitrate ion, which is here higher by about 30 cm^{-1} than in the rest of the experiments; this fact and the small peak appearing at 1261 cm^{-1} (which is also observed by Ritzhaupt and Devlin[6]) suggest that the sample is contaminated by some dihydrate. In refs 12, 13, 15, and 16, the peak at 1119 cm^{-1} is absent from the spectrum. In a recent work, Tisdale et al.[25] have observed that this peak tends to disappear when the sample is annealed at temperatures higher than 175 K. As in the previous cases, Tso and Leu do not attribute this peak to the ν_2 bending of H_3O^+, but to the symmetric stretch of NO_3^-.

From the previous discussion it is clear that there are some discrepancies between the IR spectra of nitric acid hydrates measured by different research groups. Some of these discrepancies have been attributed by Niedziela et al.[22] to the differences in the nature of the sample. These authors suggest that the spectra of thin films are inevitably affected by the substrate on which they are deposited and question thus their usefulness as models of the surface of the particles present in polar stratospheric clouds. According to this view, only the aerosol spectra are representative of unperturbed NAD and NAT. In support of their argument, Niedziela et al. show peculiarities of the RAIR spectrum of an ultrathin film of NAD reported by Koch et al.,[18] which presents a prominent peak at 1182 cm^{-1}, corresponding to the ν_2 mode of water, and extremely weak absorptions at the $\nu_3(NO_3^-)$ and $\nu_4(H_3O^+)$ frequencies, in contrast with other NAD spectra obtained either in thin film transmission[13] or in aerosols.[22,23] However, this comparison must be taken with care since the great disparity between the ultrathin film RAIR spectrum and the rest is due to well-known effects, namely, to the fact that vibrations whose dipole moment change is parallel to the surface cannot be observed and those with a dipole moment change perpendicular to the surface can give rise to an enhanced absorption due to the effects of the valence electrons of the metallic substrate. From the observed spectrum, Koch et al. concluded that the substrate has indeed an influence causing the preferential orientation of the H_3O^+ and NO_3^- C_3 axes perpendicular to the surface. These substrate effects are, however, restricted to the close vicinity of the surface and tend to disappear with increasing thickness. In fact, the NAD and NAT RAIR spectra of 100 nm films,[18] are the only cases in which they are so marked.

Leaving aside the spectra of ultrathin films, there is an overall similarity among the measurements of the rest of the literature with a reasonable accordance in the location of the main absorption features, but sometimes with significant differences in the relative absorption intensities. The measurements of the present work correspond to thicker layers (of the order of micrometers) and are much closer in appearance to those recorded in transmission or to the extinction spectra of aerosols than to those of Koch et al.[18] However, some effects associated with the reflection−absorption technique cannot be excluded. In general, in the RAIR spectra,[15,16,19] the absorbances corresponding to the wavenumber region beyond 2000 cm^{-1} (stretching vibrations of H_2O and H_3O^+) are higher than those measured in transmission or in aerosols, as compared with the lower wavenumber peaks (vibrations of NO_3^- and bending motions of H_3O^+). But even within the RAIR spectra of comparatively "thick"(μm) hydrate layers, there are appreciable variations. The spectra of the present work resemble globally more those of ref 19 than those of refs 15 and 16.

As pointed out recently by Tisdale et al.,[25] many different factors may affect the spectra of the nitric acid hydrates; type of sample, temperature of deposition, and temperature and time of annealing may all have an influence in the crystallization procedure modifying the defect abundance or the film stoichiometry. In addition, according to these authors, the possible existence of more than one crystal structure in the case of NAD or of birefringence in the NAT crystals might contribute to the disparities observed in the published spectra.

Conclusions

By means of high level ab initio calculations, we have found that the nitric acid/water complexes, up to three water units, are thermodynamically stable species. A first water unit is linked by hydrogen bonding to the H atom of the acid, and this is always the strongest bond of this type in these clusters. Successive hydrogen bondings are formed between a H atom of H_2O and the O atom of the next water unit. The mono- and dihydrate are basically planar, with one or two O−H bonds pointing alternatively up or down the plane of the molecular frame. The second water molecule in the dihydrate stabilizes the structure by a new, weaker hydrogen bond with another one of the oxygen atoms of the nitric. A similar situation occurs for the trihydrate upon addition of a third water molecule. The bond linking this third water unit to the nitric frame becomes stronger, although the trihydrate is not planar. In this complex, the four molecular units have structures which are, consecutively, closer to ionic NO_3^- and H_3O^+ for the first two, and like slightly distorted H_2O neutral species, for the next ones, in a comparatively similar way to the crystalline structure of the trihydrate. A second stable structure is found for this species, with the three water units closing in around the N−O3 bond, which is slightly less favorable energetically than the first alternative. The main features of the predicted infrared spectra of the complexes are a very strong O3−H1 stretch mode, shifted to the red for the larger clusters, strong O−H stretching bands corresponding to the excitation of single in-plane O−H bonds of the water units, and fairly stable medium intensity bands for the HNO_3 bend and NO_2 symmetric stretch.

The spectra of the crystalline hydrates were recorded using the RAIR technique on films with a thickness of the order of micrometerss deposited as amorphous solids on a cold Al plate, and then annealed in order to induce crystallization. The spectra exhibit a noteworthy red shift in the stretching frequencies of the H_2O molecules and H_3O^+ ions with respect to the values calculated for the isolated species. This red shift, due to hydrogen bonding in the solid, is in agreement with the available literature data. There is a good accordance in the main features of the various published spectra, but there is not unanimity in the details. The present spectra are similar (though not identical) to those obtained by other groups using the RAIR technique on films of comparable thickness. An overall good agreement, albeit with appreciable differences, is also obtained with IR transmission spectra of thin films and extinction spectra of aerosols. The largest discrepancies with previous measurements are found with the RAIR spectra of ultrathin films ($\approx$100 nm) which seem to be markedly affected by substrate effects. Theoretical calculations of the IR spectra of the solid hydrates have been performed by two groups for the mono- and trihydrate, respectively, and although these calculations provide some insight into the vibrational motions inside the crystal they are at present insufficient to decide on the detailed peak assignment or on the relative absorption intensities. This fact, together with the variability existing in the literature spectra, warrants further theoretical and experimental studies on the spectroscopy and structural properties of the nitric acid hydrates.

Note Added in Proof. While this paper was in the process of revision, we became aware of an article by McCurdy et al,[41] in which the nitric acid−water complexes are also the subject of study. These authors perform an ab initio calculation of the geometrical structure of the clusters $HNO_3 \cdot (H_2O)_n$, with $n = 0-4$, at MP2 level, with an aug-cc-pVDZ basis set. This calculation is somewhat complementary to ours since we have used a DFT method and a slightly larger basis set. They quote a number of structural parameters for the species up to 3 water units, which are in good agreement, in general, with the values determined in the present investigation. They also give the calculated harmonic frequencies for some of the clusters. Whereas the vibrations of the water units have values similar to ours, the frequency of the stretching vibrations of the nitric acid unit are systematically higher than those determined in this work. Similarly, the binding energies calculated by McCurdy et al. are about 10−15% larger than those reported in the present work, which match perfectly the value of Tao et al.[2] for the monohydrate. These effects may be due to the small differences in the optimized geometries plus the use of a shorter basis set in ref 41. More encouraging, however, is the coincidence in finding an almost constant increase in the binding energy of the clusters when going from one to three water molecules, a result which was already discussed above. McCurdy et al. report also the infrared spectra of argon matrixes of mixtures of nitric acid and water at two different concentration ratios, and assign them by reference to the theoretical predictions. The authors discuss the presence of various clusters within each matrix, and the impossibility of creating matrixes of single species. The matrix spectra are not comparable to the spectra of the crystals presented in our work. Some of the remaining problems in the assignment of the spectra of these species can benefit from the concurrence of these two investigations.

Acknowledgment. This investigation has been funded by the Spanish Ministry of Science and Technology, Projects REN2000-1557 and PB97-0268-C02. We are grateful to J. M. Castillo and J. Rodríguez for help in the experimental setup.

References and Notes

(1) Canagaratna, M.; Phillips, J. A.; Ott, M. E.; Leopold, K. R. *J. Phys. Chem. A* **1998**, *102*, 1489.
(2) Tao, F.-M.; Higgins, K.; Klemperer, W.; Nelson, D. D. *Geophys. Res. Lett.* **1996**, *23*, 1797.
(3) Carl, S. A.; Ingham, T.; Moortgat, G. K.; Crowley, J. N. *Chem. Phys. Lett.* **2001**, *341*, 93.
(4) Hamill, P.; Turco, R. P.; Toon, O. B. *J. Atmos. Chem.* **1988**, *7*, 287.
(5) Lebrun, N.; Mahe, F.; Lamiot, J.; Foulon, M.; Petit, J.; Prevost, D. *Acta Crystallogr.* **2001**, *B57*, 27.
(6) Ritzhaupt, G.; Devlin, J. P. *J. Phys. Chem.* **1991**, *95*, 90.
(7) Koller, J.; Hadzi, D. *J. Mol. Struct.* **1991**, *247*, 225.
(8) Tóth, G. *J. Phys. Chem. A* **1997**, *101*, 8871.
(9) Sullivan, D. M.; Bagchi, K.; Tuckerman, M. E.; Klein, M. I. *J. Phys. Chem. A* **1999**, *103*, 8678.
(10) Staikova, M.; Donaldson, D. J. *Phys. Chem. Chem. Phys.* **2001**, *3*, 1999.
(11) Smith, R. H.; Leu, M.-T.; Keyser, L. F. *J. Chem. Phys.* **1991**, *95*, 5924.
(12) Koehler, B. G.; Middlebrook, A. M.; Tolbert, M. A. *J. Geophys. Res.* **1992**, *97*, 8065.
(13) Tolbert, M. A.; Koehler, B. G.; Middlebrook, A. M. *Spectrochim. Acta* **1992**, *48A*, 130.
(14) Barton, N.; Rowland, B.; Devlin, J. P. *J. Phys. Chem.* **1993**, *97*, 5848.
(15) Schrems, O.; Peil, S. *Heterogeneous and Homogeneous Chemistry of ClO_y, BrO_y, and NO_y Compounds on Polar Stratospheric Cloud Mimics. CEC Report for STEP Programme CT-90-0071*, 1993. The RAIR spectra of the nitric acid hydrates are shown in Figure 2 of Sodeau, J. R.

Atmospheric Cryochemistry. In *Spectroscopy in Enviromental Science*; Clark, R. H. J., Lester, R. E., Eds.; John Wiley and Sons: New York, 1995.
(16) Peil, S.; Seisel, S.; Schrems, O. *J. Mol. Struct.* **1995**, *348*, 449.
(17) Richwine, J. L.; Clapp, M. L.; Miller, R. E.; Worsnop, D. R. *Geophys. Res. Lett.* **1995**, *22*, 2625.
(18) Koch, T. G.; Holmes, N. S.; Roddis, T. B.; Sodeau, J. R. *J. Chem. Soc., Faraday Trans*. **1996**, *92*, 4787.
(19) Tso, T.-L.; Leu, M.-T. *Anal. Sci*. **1996**, *12*, 615.
(20) Dieselkamp, R. S.; Anthony, S. E.; Prenni, A. J.; Onasch, T. B.; Tolbert, M. A. *J. Phys. Chem.* **1996**, *100*, 9127.
(21) Tisdale, R. T.; Middlebrook, A. M.; Prenni, A. J.; Tolbert, M. A. *J. Phys. Chem. A* **1997**, *101*, 2112.
(22) Niedziela, R. F.; Miller, R. E.; Worsnop, D. R. *J. Phys. Chem. A.* **1998**, *102*, 6477.
(23) Bertram, A. K.; Sloan, J. J. *J. Geophys. Res.* **1998**, *103*, 3553.
(24) Bertram, A. K.; Sloan, J. J. *J. Geophys. Res.* **1998**, *103*, 13265.
(25) Tisdale, R. T.; Prenni, A. J.; Iraci, L. T.; Tolbert, M. A.; Toon, O. B. *Geophys. Res. Lett.* **1999**, *26*, 707.
(26) Toon, O. B.; Tolbert, M. A.; Koehler, B. G.; Middlebrook, A. M.; Jordan, J. *J. Geophys. Res.* **1994**, *99*, 25631.
(27) Nielsen, I. M. B.; Seidl, E. T.; Janssen, C. L. *J. Chem. Phys.* **1999**, *110*, 9435.
(28) Gálvez, O.; Gómez, P. C.; Pacios, L. F. *Chem. Phys. Lett.* **2001**, *337*, 263.
(29) Gálvez, O.; Gómez, P. C.; Pacios, L. F. *J. Chem. Phys.* **2001**, *115*, 11166.
(30) Frisch, M. J.; Trucks, G. W.; Schlegel, H. B.; Scuseria, G. E.; Robb, M. A.; Cheeseman, J. R.; Zakrzewski, V. G.; Montgomery, J. A., Jr.; Stratmann, R. E.; Burant, J. C.; Dapprich, S.; Millam, J. M.; Daniels, A. D.; Kudin, K. N.; Strain, M. C.; Farkas, O.; Tomasi, J.; Barone, V.; Cossi, M.; Cammi, R.; Mennucci, B.; Pomelli, C.; Adamo, C.; Clifford, S.; Ochterski, J.; Petersson, G. A.; Ayala, P. Y.; Cui, Q.; Morokuma, K.; Malick, D. K.; Rabuck, A. D.; Raghavachari, K.; Foresman, J. B.; Cioslowski, J.; Ortiz, J. V.; Baboul, A. G.; Stefanov, B. B.; Liu, G.; Liashenko, A.; Piskorz, P.; Komaromi, I.; Gomperts, R.; Martin, R. L.; Fox, D. J.; Keith, T.; Al-Laham, M. A.; Peng, C. Y.; Nanayakkara, A.; Gonzalez, C.; Challacombe, M.; Gill, P. M. W.; Johnson, B.; Chen, W.; Wong, M. W.; Andres, J. L.; Head-Gordon, M.; Replogle, E. S.; Pople, J. A. *GAUSSIAN98 (G98W)*; Gaussian Inc.: Pittsburgh, PA, 1998.
(31) Donaldson, D. J. *J. Phys. Chem. A* **1999**, *103*, 62.
(32) Carrasco, E.; Castillo, J. M.; Escribano, R.; Herrero, V. J.; Moreno, M. A.; Rodríguez, J. *Rev. Sci. Instrum.* **2002**, *73*, 3469.
(33) Clavelin, J. L.; Mirabel, P. *J. Chim. Phys.-Phys. Chim. Biol.* **1979**, *76*, 533.
(34) Hanson, D.; Mauersberger, K. *J. Phys. Chem.* **1988**, *92*, 6167.
(35) Brown, D. E.; George, S. M.; Huang, C.; Wong, E. K. L.; Rider, K. B.; Smith, R. S.; Kay, B. D. *J. Phys. Chem.* **1996**, *100*, 4988.
(36) Taesler, I.; Delaplane, R. G.; Olovsson, I. *Acta Crystallogr*. **1975**, *B31*, 1489.
(37) Ortiz-Repiso, M.; Escribano, R.; Gómez, P. C. *J. Phys. Chem. A* **2000**, *104*, 600.
(38) Delaplane, R. G.; Taesler, I.; Olovsson, I. *Acta Crystallogr*. **1975**, *B31*, 1486.
(39) Begemann, M. H.; Gudemann, C. S.; Pfaff, J.; Saykally, R. J. *Phys. Rev. Lett.* **1983**, *51*, 54.
(40) The assignment and numbering of the normal modes of the hydronium and nitrate ions follows the disposition shown in Fig. 4 of ref 18.
(41) McCurdy, P. R.; Hess, W. P.; Xantheas, S. *J. Phys. Chem. A* **2002**, *106*, 7628.